Spatial density profile of electrons near the LaAlO[3]/SrTiO[3] heterointerface revealed by time-resolved photoluminescence spectroscopy

AUTHOR(S):

Yamada, Yasuhiro; Sato, Hiroki K.; Hikita, Yasuyuki; Hwang, Harold Y.; Kanemitsu, Yoshihiko

CITATION:

Yamada, Yasuhiro ...[et al]. Spatial density profile of electrons near the LaAlO[3]/SrTiO[3] heterointerface revealed by time-resolved photoluminescence spectroscopy. Applied Physics Letters 2014, 104(15): 151907.

ISSUE DATE:

2014-04-14

URL:

http://hdl.handle.net/2433/185716

Spatial density profile of electrons near the LaAlO3/SrTiO3 heterointerface revealed by time-resolved photoluminescence spectroscopy

Yasuhiro Yamada, Hiroki K. Sato, Yasuyuki Hikita, Harold Y. Hwang, and Yoshihiko Kanemitsu

Citation: Applied Physics Letters **104**, 151907 (2014); doi: 10.1063/1.4872171
View online: http://dx.doi.org/10.1063/1.4872171
View Table of Contents: http://scitation.aip.org/content/aip/journal/apl/104/15?ver=pdfcov
Published by the AIP Publishing

APPLIED PHYSICS LETTERS **104**, 151907 (2014)

Spatial density profile of electrons near the $LaAlO_3/SrTiO_3$ heterointerface revealed by time-resolved photoluminescence spectroscopy

Yasuhiro Yamada,[1,a)] Hiroki K. Sato,[2,3] Yasuyuki Hikita,[2] Harold Y. Hwang,[2,4] and Yoshihiko Kanemitsu[1]

[1]*Institute for Chemical Research, Kyoto University, Uji, Kyoto 611-0011, Japan*
[2]*SLAC National Accelerator Laboratory, Stanford Institute for Materials and Energy Sciences, Menlo Park, California 94025, USA*
[3]*Department of Advanced Materials Science, The University of Tokyo, Kashiwa, Chiba 277-8561, Japan*
[4]*Geballe Laboratory for Advanced Materials, Department of Applied Physics, Stanford University, Stanford, California 94305, USA*

(Received 26 March 2014; accepted 10 April 2014; published online 17 April 2014)

The depth profile of the electron density near the $LaAlO_3/SrTiO_3$ heterointerface has been studied by means of time-resolved photoluminescence (PL) spectroscopy. A broad blue PL band is observed at 2.9 eV, originating from the two-carrier radiative recombination of interface-induced electrons and photoexcited holes. The PL lifetime of $LaAlO_3/SrTiO_3$ heterointerface is dominated by the three-carrier Auger recombination of electrons and holes and is sensitive to electron density. We tuned the probing depth by changing the excitation photon energy and evaluated the carrier-density profile using the relation between the carrier density and the PL lifetime. Our non-contact probe method based on PL spectroscopy indicates that the carriers are confined within several nanometers in depth near the $LaAlO_3/SrTiO_3$ heterostructures. © *2014 AIP Publishing LLC*. [http://dx.doi.org/10.1063/1.4872171]

Recent progress in layer-by-layer thin-film growth techniques has enabled the precise design of heterostructures that possess unique functionalities beyond bulk crystals.[1] Since the discovery of a quasi-two-dimensional electron gas (2DEG) system formed at the $LaAlO_3/SrTiO_3$ (LAO/STO) heterointerface,[2] oxide heterostructures have attracted a great deal of attention both from the viewpoints of fundamental physics and device applications.[3–5] Electrical conduction appears at an AlO_2–LaO/TiO_2 interface with a $LaAlO_3$ layer above the critical thickness (~4 unit cells). Electrons are confined within a few nanometers in depth on the $SrTiO_3$ side,[6,7] and the interface carriers display a variety of fascinating properties.[8–14] These findings stimulate the development of electronic devices based on oxide heterointerfaces, such as field effect transistors and nonvolatile memories.[15–18] For further development of devices based on the oxide heterointerface, we must unveil the physics behind the 2DEG formation.

The formation mechanism of 2DEG has been discussed in terms of polarization catastrophe (charge transfer from the LAO surface to the interface), atom interdiffusion, and oxygen vacancies induced at the interface.[8,19–21] It is believed that each of them can play a critical role in 2DEG formation depending on fabrication conditions.[18,19] To discuss the 2DEG formation mechanism, it is important to study the depth profile of the interface carriers, which requires developing a noncontact and non-destructive probe method to minimize the influence of the measurement on the electronic state.

We have previously studied the nature of carriers and carrier recombination dynamics of bulk $SrTiO_3$ crystals by means of optical probe techniques, such as time-resolved photoluminescence (PL) and transient absorption (TA) spectroscopy.[22–26] Strongly photoexcited or electron-doped $SrTiO_3$ shows a broad blue PL band at room temperature because of the radiative recombination of electrons and holes. The PL dynamics of $SrTiO_3$ can be explained on the basis of a simple model that includes nonradiative Auger recombination involving three carriers such as electron-electon-hole.[22,23,27] Because we have quantitatively evaluated the Auger recombination rate of $SrTiO_3$, whereby the carrier dynamics depend on the carrier density, the analysis of the PL dynamics provides the requisite information on the carrier density. Using this non-contact probe method for evaluating carrier recombination dynamics, we have demonstrated the quantitative evaluation of the spatial carrier-density profile in Ar^+-irradiated $SrTiO_3$, where the oxygen-deficient metallic surface layer exists near the surface.[26]

Here, we report the room-temperature PL decay dynamics of an *n*-type conducting LAO/STO heterointerface. With an increase in the photon energy (in other words, a decrease in the penetration depth of the excitation light), the PL decay time decreases. This result means that the Auger recombination rate is enhanced due to the high carrier density near the interface. The PL dynamics is converted into the depth profile of the interface carrier density using a genetic-algorithm (GA)–like analysis, where a set of trial functions asymptotically approaches the actual carrier-density profile. Our non-contact probe technique provides an independent method to probe the carrier density distribution at the interface. In addition, the analysis method proposed here offers a powerful tool for interpreting PL dynamics in inhomogeneous materials.

We used chemically electron-doped $SrTiO_3$ single crystals [$SrNb_xTi_{1-x}O_3$ ($x = 0.001$): Nb-STO] (Furuuchi Chemical Co.) and *n*-type LAO/STO heterostructures. The LAO/STO interfaces were grown by pulsed laser deposition using a single-crystal $LaAlO_3$ target on TiO_2-terminated (100) $SrTiO_3$ single-crystal substrates. The details of the fabrication

[a)]yamada.yasuhiro.6c@kyoto-u.ac.jp

procedure have been described elsewhere.[14] Time-resolved PL spectra were measured with a time resolution of 40 ps using a streak camera and a monochromator. The excitation light source was a wavelength-tunable optical parametric amplifier system based on a regeneratively amplified mode-locked Ti:sapphire laser with a pulse duration of 150 fs and a repetition rate of 1 kHz. The excitation laser beam was used to illuminate the $LaAlO_3$ side of the sample. Because the bandgap energy of $LaAlO_3$ (~5 eV) is much higher than the excitation photon energy, no photo-absorption occurs in the $LaAlO_3$ layer, and the excitation light reaches the $SrTiO_3$ layer with negligible loss. The laser spot size on the sample surface was carefully measured using the knife-edge method. All spectroscopic measurements were carried out at room temperature.

Figure 1 shows the time-integrated PL spectra of a Nb-doped $SrTiO_3$ single crystal and an *n*-type LAO/STO heterostructure at room temperature. The excitation photon energy was 4.00 eV. The corresponding optical penetration depth is 15 nm.[28] The PL spectrum shape of the LAO/STO heterostructure shows a broad blue PL band at around 2.9 eV and is almost identical to that of the Nb-doped $SrTiO_3$ single crystal. This indicates that the origin of the PL of the LAO/STO heterointerface is the same as that of an electron-doped $SrTiO_3$ single crystal.

As we have previously reported, the blue room-temperature PL of $SrTiO_3$ stems from the two-carrier radiative recombination of electrons and holes, and the PL decay dynamics is well reproduced by the following equations considering the three-carrier Auger recombination process:[22,23,25]

$$\frac{dn}{dt}(t) = -A_n n - Bnp - C_n n^2 p - C_p np^2, \tag{1a}$$

$$\frac{dp}{dt}(t) = -A_p p - Bnp - C_n n^2 p - C_p np^2, \tag{1b}$$

$$I(t) \propto Bn(t)p(t). \tag{1c}$$

Here, $I(t)$, $n(t)$, and $p(t)$ are, respectively, the PL intensity, electron density, and hole density at time t. A_n and A_p are, respectively, the electron and hole trapping rates. B represents the two-carrier radiative recombination coefficient. The radiative recombination rate is negligibly small compared to the trapping rate and the Auger recombination rate. C_n and C_p are, respectively, the three-carrier (electron–electron–hole and electron–hole–hole) non-radiative Auger recombination coefficients. Due to the Auger recombination process, the PL decay profile of undoped $SrTiO_3$ single crystals depends strongly on the excitation power density under high-density excitation. In the case of undoped $SrTiO_3$, the electron and hole densities just after the photoexcitation are identical. Therefore, according to Eqs. (1a)–(1c), the PL intensity is approximately proportional to the square of the photoexcited carrier density.[25,26]

In electron-doped $SrTiO_3$, where the photoexcited carrier density (n) is much below the doped carrier density (N_e), Auger recombination of photoexcited holes and doped electrons is dominant, and the recombination of photoexcited electrons and hole is negligible. Therefore, in this case (where $N_e \gg n$), Eqs. (1a)–(1c) can be simplified, yielding

$$\frac{dn}{dt} = -Ap - CN_e^2 p \quad (N_e \gg n), \tag{2a}$$

$$I(t) \propto BN_e p(t). \tag{2b}$$

The PL intensity increases linearly with the excitation density, and the PL decay profile is independent of the excitation density. According to Eqs. (2a) and (2b), the PL decay shows exponential decay, and the decay rate ($A + CN_e^2$) is determined by the carrier density. In other words, we can estimate the doped-carrier density of $SrTiO_3$ by means of the PL dynamics. By altering the excitation photon energy, we can change the probed region of the sample, as schematically illustrated in Fig. 2(a), because the penetration depth is strongly dependent on the excitation photon energy.[26,28,29] Therefore, we can make a quantitative evaluation of the spatial carrier-density profile from the PL decay dynamics under excitation at various excitation energies.

Figure 2(b) shows the PL dynamics of the LAO/STO heterostructure monitored at 2.8 eV under different excitation densities. The PL intensity was normalized and offset for clarity. The excitation photon energy was 4.00 eV. The

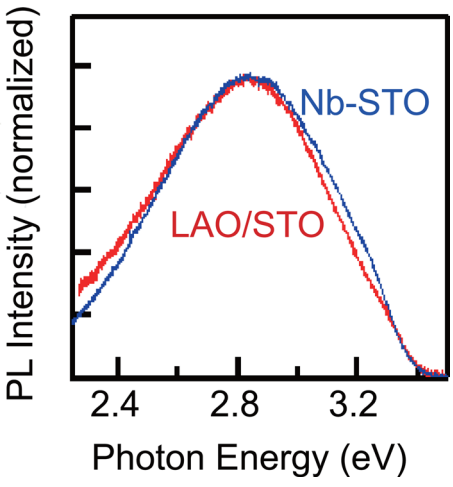

FIG. 1. PL spectra of the Nb-doped STO (Nb-STO) single crystal and the LAO/STO heterostructure.

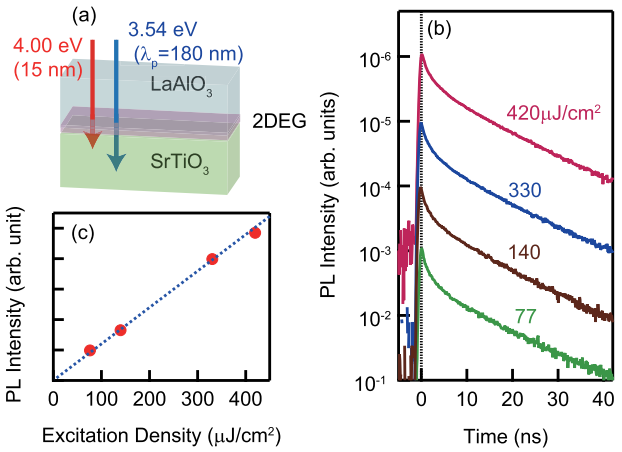

FIG. 2. (a) Schematic illustration of the probing depth for the different excitation energy values. (b) PL dynamics of the LAO/STO heterostructure under different excitation intensities. Excitation photon energy was 4.00 eV. (c) Excitation-density dependence of the time-integrated PL intensity.

PL dynamics show nonexponential decay profiles, which are almost independent of excitation density below 420 μJ/cm^2. The time-integrated PL intensity is linearly dependent on the excitation density, as shown in Fig. 2(c). The carrier recombination dynamics of the LAO/STO heterostructures are completely different from those of undoped $SrTiO_3$. These results suggest that both the radiative and nonradiative recombination of photoexcited electrons and photoexcited holes are negligibly small below 420 μJ/cm^2. In the experiment used to collect the data shown in Fig. 3, the excitation density was below 420 μJ/cm^2, where the PL decay profile is independent of excitation density.

Figure 3(a) shows the PL dynamics of the LAO/STO heterostructure under different excitation photon energies. The PL decay curves show non-exponential profiles, indicating the non-uniform spatial distribution of carriers. With an increase in photon energy (or a decrease in penetration depth), the PL decay becomes faster. This indicates a higher electron density near the interface.

In the sample with a large spatial distribution of carriers, the temporal variation of the PL is expressed as

$$I(t) \propto B \int_0^\infty N_e(z) p(z,t) dz, \tag{3}$$

where $p(z,t)$ is given by Eqs. (2a) and (2b), $p(z,0) = p_0 \exp(-\alpha z)$, and $1/\alpha$ is the optical penetration depth. Here, we used the A and C coefficient values from undoped $SrTiO_3$ single crystals.[23] Note that we assume here that photoexcited holes are immobile because of their highly localized nature. We can easily calculate the excitation-energy–dependent PL dynamics based on the depth profile of the carrier density using Eqs. (2a), (2b), and (3). However, the inverse calculation is difficult: in general, it is difficult to estimate the integrand from integrated values by solving integral equation such as Eq. (3).

Here, we used a GA-like approach to derive the carrier-density profile from the PL dynamics. The fundamental procedures of this GA-like analysis are as follows: (i) A set of trial functions for carrier-density profiles was prepared. Our initial trial functions are exponential functions with different decay constants. (ii) The PL dynamics for the trial functions were calculated by using Eq. (3), and the difference between the experimental and calculated results was estimated. (iii) Some unmatched trial functions are replaced with new trial functions with a certain probability. Some of the new trial functions (created through a process called "mutation") are completely different from the existing trial functions, and the others are created by a combination of two well-matched trial functions (a process called "crossover"). (iv) After performing steps (ii)–(iv) repeatedly, the best-matched trial function is finally selected as a solution for Eq. (3). The solid curves show the calculated results based on Eqs. (2a), (2b), and (3), which reproduce the experimental data well.

The calculated depth profile of the carrier density is shown in Fig. 3(b). The maximum carrier density was 3 $\times$ 10^{20} cm^{-3} at the interface, and most of the carriers are confined within a 5-nm interface region. Although it is difficult to determine the carrier density below several nanometers accurately, taking the penetration depth of 15 nm for 4.00 eV into consideration, we can conclude that most of the carriers are strongly confined within several nanometers of the interface. In addition, by integrating the calculated depth profile of carriers between 0 and 15 nm, we obtain two-dimensional carrier density $N_{2D} \sim 2 \times 10^{14}$ cm^{-2}, which is quite close to $e/2$ per unit cell ($N_{2D} \sim 3 \times 10^{14}$ cm^{-2}) derived from the polar catastrophe model.[2] This result suggests that the electronic reconstruction due to the polar catastrophe mechanism at the interface is the dominant source of the interface conductivity. On the other hand, carriers still exist at depths of several tens of nanometers, which indicate that there are weak contributions to the interface conductivity from other factors such as oxygen defects in this sample. This weak component of the carrier density spreads to depths of over 1 μm in our calculation (see the inset of Fig. 3). However, it should be noted that the carrier density component at depths of over 1 μm is not well reproduced by our calculation because of the low accuracy of the calculation in this region.

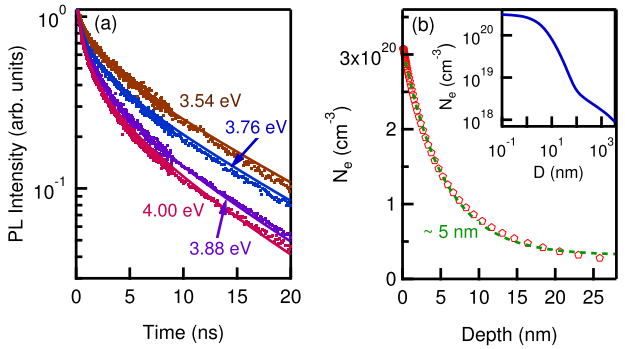

FIG. 3. (a) PL dynamics of LAO/STO under excitation photon energies of 4.00, 3.88, 3.76, and 3.54 eV. The corresponding penetration depths for 4.00, 3.88, 3.76, and 3.54-eV excitation photon energies are 15, 24, 40, and 180 nm, respectively (from Ref. 28). The solid curves represent the calculated PL dynamics. (b) Calculated depth profile of carriers near the LAO/STO heterostructure. The dotted curve shows the fitting result by a single-exponential function. The inset shows the depth profile in a log-log plot.

In conclusion, we performed a PL study of LAO/STO heterostructures. The PL spectrum of LAO/STO shows a broad blue PL band that is identical to that of the electron-doped $SrTiO_3$ single crystal. The PL decay of LAO/STO shows a nonexponential profile, which indicates an inhomogeneous spatial profile of the carriers. From PL decay analyses, we obtained the depth profile of the interface carriers. This result clarified that most of the carriers are confined within several nanometers of the interface on the $SrTiO_3$ side and that there is also a weak contribution from a component with large spatial extent, which may be due to oxygen defects.

Part of this work at Kyoto University was supported by KAKENHI (No. 24740202), the Sumitomo Electric Industries Group CSR Foundation, and JST-CREST. H.K.S., Y.H., and H.Y.H. acknowledge support from the Department of Energy, Office of Basic Energy Sciences, Materials Sciences and Engineering Division, under Contract No. DE-AC02-76SF00515. H.K.S. acknowledges partial support from the ONR-MURI No. N00014-12-1-0976.

[1]D. G. Schlom, L. Q. Chen, X. Q. Pan, A. Schmehl, and M. A. Zurbuchen, J. Am. Ceram. Soc. **91**, 2429 (2008).

[2]A. Ohtomo and H. Y. Hwang, Nature (London) **427**, 423 (2004).
[3]H. Y. Hwang, Y. Iwasa, M. Kawasaki, B. Keimer, N. Nagaosa, and Y. Tokura, Nature Mater. **11**, 103 (2012).
[4]J. Mannhart and D. G. Schlom, Science **327**, 1607 (2010).
[5]P. Zubko, S. Gariglio, M. Gabay, P. Ghosez, and J. M. Triscone, Annu. Rev. Condens. Matter Phys. **2**, 141 (2011).
[6]K. Yoshimatsu, R. Yasuhara, H. Kumigashira, and M. Oshima, Phys. Rev. Lett. **101**, 026802 (2008).
[7]M. Basletic, J.-L. Maurice, C. Carrétéro, G. Herranz, O. Copie, M. Bibes, É. Jacquet, K. Bouzehouane, S. Fusil, and A. Barthélémy, Nature Mater. **7**, 621 (2008).
[8]N. Nakagawa, H. Y. Hwang, and D. A. Muller, Nature Mater. **5**, 204 (2006).
[9]S. Thiel, G. Hammerl, A. Schmehl, C. W. Schneider, and J. Mannhart, Science **313**, 1942 (2006).
[10]N. Reyren, S. Thiel, A. D. Cavigla, L. Koukoutis, G. Hammerl, C. Richter, C. W. Schneider, T. Kopp, A. S. Rüetschi, D. Jaccard, M. Gabay, D. A. Muller, J. M. Triscone, and J. Mannhart, Science **317**, 1196 (2007).
[11]A. D. Caviglia, S. Gariglio, C. Cancellieri, B. Sacépé, A. Fête, N. Reyren, M. Gabay, A. F. Morpurgo, and J.-M. Triscone, Phys. Rev. Lett. **105**, 236802 (2010).
[12]R. Yamamoto, C. Bell, Y. Hikita, H. Y. Hwang, H. Nakamura, T. Kimura, and Y. Wakabayashi, Phys. Rev. Lett. **107**, 036104 (2011).
[13]J. A. Bert, K. C. Nowack, B. Kalisky, H. Noad, J. R. Kirtley, C. Bell, H. K. Sato, M. Hosoda, Y. Hikita, H. Y. Hwang, and K. A. Moler, Phys. Rev. B **86**, 060503(R) (2012).
[14]Y. Yamada, H. K. Sato, Y. Hikita, H. Y. Hwang, and Y. Kanemitsu, Phys. Rev. Lett. **111**, 047403 (2013).
[15]B. Förg, C. Richter, and J. Mannhart, Appl. Phys. Lett. **100**, 053506 (2012).
[16]C. Cen, S. Thiel, J. Mannhart, and J. Levy, Science **323**, 1026 (2009).
[17]D. Stornaiuolo, S. Gariglio, N. J. G. Couto, A. Fête, A. D. Caviglia, G. Seyfarth, D. Jaccard, A. F. Morpurgo, and J.-M. Triscone, Appl. Phys. Lett. **101**, 222601 (2012).
[18]M. Hosoda, Y. Hikita, H. Y. Hwang, and C. Bell, Appl. Phys. Lett. **103**, 103507 (2013).
[19]G. Herranz, M. Basletic, M. Bibes, C. Carretero, E. Tafra, E. Jacquet, K. Bouzehouane, C. Deranlot, A. Hamzic, J.-M. Broto, A. Barthelemy, and A. Fert, Phys. Rev. Lett. **98**, 216803 (2007).
[20]A. Kalabukhov, R. Gunnarsson, J. Borjesson, E. Olsson, T. Claeson, and D. Winkler, Phys. Rev. B **75**, 121404 (2007).
[21]P. R. Willmott, S. A. Pauli, R. Herger, C. M. Schlepütz, D. Martoccia, B. D. Patterson, B. Delley, R. Clarke, D. Kumah, C. Cionca, and Y. Yacoby, Phys. Rev. Lett. **99**, 155502 (2007).
[22]H. Yasuda and Y. Kanemitsu, Phys. Rev. B **77**, 193202 (2008).
[23]Y. Yamada, H. Yasuda, T. Tayagaki, and Y. Kanemitsu, Appl. Phys. Lett. **95**, 121112 (2009).
[24]Y. Yamada and Y. Kanemitsu, Phys. Rev. B **82**, 121103(R) (2010).
[25]Y. Yamada, H. Yasuda, T. Tayagaki, and Y. Kanemitsu, Phys. Rev. Lett. **102**, 247401 (2009).
[26]H. Yasuda, Y. Yamada, T. Tayagaki, and Y. Kanemitsu, Phys. Rev. B **78**, 233202 (2008).
[27]P. T. Landsberg, *Recombination in Semiconductors* (Cambridge University Press, Cambridge, 1991).
[28]M. Cardona, Phys. Rev. **140**, A651 (1965).
[29]Y. Kozuka, Y. Hikita, T. Susaki, and H. Y. Hwang, Phys. Rev. B **76**, 085129 (2007).